Imaging Agents

DOI: 10.1002/anie.201203031

Near-Infrared Emitting Radioactive Gold Nanoparticles with Molecular Pharmacokinetics**

Chen Zhou, Guiyang Hao, Patrick Thomas, Jinbin Liu, Mengxiao Yu, Shasha Sun, Orhan K. Öz, Xiankai Sun, and Jie Zheng**

Contrast agents used in clinics often exhibit the following pharmacokinetics: rapid diffusion (short distribution half-life $t_{1/2\alpha}$), relatively long blood circulation time (long elimination half-life $t_{1/2\beta}$), and little nonspecific accumulation in the body (renal clearable) after systemic administration.[1] These specific pharmacokinetic features not only ensure the success of clinical imaging processes but also minimize the potential health hazards caused by the introduction of contrast agents. For example, ^{99m}Tc-SQ30217 (a single-photon emission computed tomography (SPECT) imaging agent),[2] ^{18}F-labeled fluoroacetate ([^{18}F]FAc) (a highly potential positron emission tomography (PET) imaging agent),[3] and Iomeprol (a commercially available X-ray computed tomography (CT) contrast agent)[4] exhibit a $t_{1/2\alpha}$ of about 1.2 min, 9.0 min, and 16.2 min, and a $t_{1/2\beta}$ of about 10.1 h, 11.3 h, and 2.34 h after intravenous (IV) injection, respectively.

While these contrast agents based on small molecules have been widely used or hold great potential in the clinics, one major limitation is that they are only suitable for single modality imaging. As a result, the strengths of different imaging techniques are hardly integrated together for better disease management. To address this challenge, significant efforts have been devoted to developing multimodal imaging probes in the past decades.[5] One general approach is to integrate different functional small molecules together using elegant synthetic strategies.[5d,6] For example, Banerjee et al. reported a small-molecule-based dual modality SPECT/near-infrared fluorescence (NIRF) imaging agent, which shows high and specific uptake in prostate-specific membrane antigen (PSMA) positive xenografts and excellent pharmacokinetics for targeting PSMA in vivo.[5d] As a parallel direction, nanoparticle (NP) based multimodal imaging probes have also attracted great attention because inorganic NPs typically exhibit large surface/volume ratios, tunable and diverse material properties.[5e,7] For instance, radioactive quantum dots (QDs) labelled with ^{64}Cu have been used in fluorescence and PET imaging.[8] Lin et al. developed robust luminescent and paramagnetic hybrid silica NPs for optical and magnetic resonance imaging (MRI), respectively.[5a] Gold NPs (AuNPs) not only can serve as nonphotobleaching emitters in dark-field, Raman, and photothermal imaging in vitro,[9] but also can be used to enhance contrasts of photoacoustics and computed tomography imaging in vivo.[10] While these exciting biomedical applications are continuously driving the emergence of novel multimodal nanoprobes, inorganic NPs often exhibit pharmacokinetics different from those of small-molecule contrast agents. For instance, carbon nanotubes[11] and iron oxide NPs[12] only shown a short first-order exponential blood circulation with half-lives of about 1.0 h and about 0.12 h after IV injection, respectively. In addition, reticuloendothelial system (RES) organs often rapidly sequester these nanostructures, resulting in slow RES clearance processes and potential health hazards.[7g,9c,13] These limitations in pharmacokinetics of NPs significantly hamper their clinical applications. Thus, it is highly desirable to develop nanoprobes that possess diverse material properties suitable for different imaging techniques and also exhibit optimal in vivo pharmacokinetics.

The biodistribution, renal clearance, and pharmacokinetics of nanoprobes mainly depend on their particle sizes and surfaces.[14] For example, multifunctional silica-based particles smaller than 5 nm can effectively evade uptake by the reticulo-endothelial system (RES).[14e] In addition to the particle size/hydrodynamic diameter, the surface also plays an important role in renal clearance of NPs. Our recent investigations[15] showed that glutathione, a small tri-peptide, can serve as an effective surface ligand to minimize nonspecific accumulation of luminescent AuNPs in the RES organs and enabled more than 50% of the glutathione-coated luminescent AuNPs (GS-AuNPs) to be cleared out of the body through the urinary system within 48 h.[15b] However, their pharmacokinetics in comparison with clinical contrast agents (short $t_{1/2\alpha}$ and relatively long $t_{1/2\beta}$) remains unexplored.

To address these questions and potential challenges in biomedical applications of luminescent AuNPs, we herein report a one-step synthesis of NIR-emitting radioactive GS-coated [^{198}Au]AuNPs (GS-[^{198}Au]AuNPs) with quantitative labeling yield and 100% purity, which allow us to readily quantify the biodistributions with the ^{198}Au signal at different time points post injection (p.i.). The pharmacokinetic studies

[*] C. Zhou, Dr. J. Liu, Dr. M. Yu, S. Sun, Prof. Dr. J. Zheng
Department of Chemistry, The University of Texas at Dallas
800 W. Campbell Road, Richardson, TX 75080 (USA)
E-mail: jiezheng@utdallas.edu
Homepage: http://www.utdallas.edu/~jiezheng
Dr. G. Hao, P. Thomas, Prof. Dr. O. K. Öz, Prof. Dr. X. Sun
Department of Radiology, The University of Texas Southwestern Medical Center
5323 Harry Hines Boulevard, Dallas, TX 75390 (USA)
E-mail: xiankai.sun@utsouthwestern.edu

[**] This work was supported in part by the NIH (grant number R21EB009853 to J.Z.), CPRIT (grant numberRP120588 J.Z. and X.S.) and the start-up fund from the University of Texas at Dallas (J.Z.). The purchase of the NanoSPECT-CT scanner was partially supported by an NIH shared instrumentation grant (grant number 1S10RR029674-01 to O.K.Ö.).

Supporting information for this article is available on the WWW under http://dx.doi.org/10.1002/anie.201203031.

indicated that these nanoprobes exhibit a rapid $t_{1/2\alpha}$ of 5.0 min, and a $t_{1/2\beta}$ of 12.7 h. This two-compartment pharmacokinetics is similar to those of the clinically available small molecule contrast agents[16] but different from those of most known nanoprobes, which often just show one-compartment kinetics.[12,14e] Surprisingly, while the energy window of the gamma emission of ^{198}Au (0.411 MeV) is suboptimal for the current SPECT scanners,[17] these NIR-emitting radioactive [^{198}Au]AuNPs can be readily detected with both SPECT imaging and fluorescence imaging techniques, implying that they might serve as dual-modality imaging probes in the future.

The synthesis of the NIR-emitting [^{198}Au]AuNPs is fairly simple and straightforward, only requiring one-step thermal reduction of ^{197}Au and radiotracer ^{198}Au ions in the presence of glutathione. The detailed synthesis and purification procedures are shown in the Supporting Information. The radiolabeling purity of ^{198}Au was assessed using radio high-performance liquid chromatography (radio-HPLC) with two detectors (UV and gamma counters), which indicated that the radiochemical purity of the GS-[^{198}Au]AuNPs was nearly 100% (Figure 1a). Figure 1b shows the mean core size distribution and hydrodynamic diameter of the synthesized GS-[^{198}Au]AuNPs around (2.6 ± 0.3) nm and (3.0 ± 0.4) nm, respectively (Figure 1c). The GS-[^{198}Au]AuNPs also exhibited NIR emission with a maximum located at 810 nm (Figure 1d). Consistent with previous studies on few-nanometer-small luminescent AuNPs coated by glutathione and many other ligands,[15a,18] the X-ray photoelectron spectroscopy (XPS) measurement showed that 39% of Au atoms in the GS-[^{198}Au]AuNPs are actually in the Au^{I} state (see Figure S1 in the Supporting Information), which formed strong Au^{I}–S bonds with the glutathione ligand. The large Stokes shifts (about 450 nm) and microsecond emission lifetimes of 0.64 μs (47%)/3.67 μs (53%) (Figure S2) suggested that NIR emission of GS-[^{198}Au]AuNPs fundamentally arises from the quantized transitions between surface states formed through hybridization of p orbitals of sulfur atoms and the sp band of surface Au^{I} atoms.[18] In addition, different from conventional similar-sized plasmonic AuNPs, GS-[^{198}Au]AuNPs display no surface plasmon absorption (Figure 1d) because a large amount of gold(I) atoms in these luminescent AuNPs failed to donate free electrons to support surface plasmons. The quantum yield of GS-[^{198}Au]AuNPs was quantified to be about 0.7% in aqueous solution, comparable to the nonradioactive NIR-emitting GS-AuNPs,[18b] suggesting the introduction of ^{198}Au has little influence on the emission property of the AuNPs.

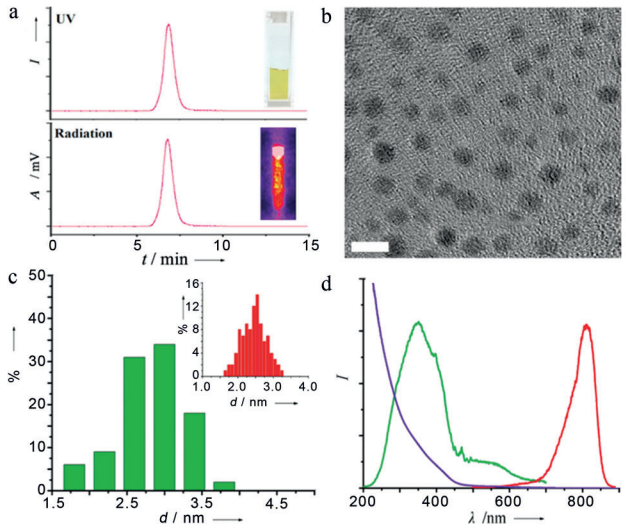

Figure 1. Characterization of glutathione-coated near-infrared (NIR) emitting radioactive AuNPs (GS-[^{198}Au]AuNPs). a) Radio high-performance liquid chromatography (radio-HPLC) showing the radiochemical purity of GS-[^{198}Au]AuNPs is 100%. Inset: Bright-field image and radiation image of GS-[^{198}Au]AuNPs. b) Typical transmission electron microscopy (TEM; scale bar = 5 nm) image of GS-[^{198}Au]AuNPs showing c) a core size of (2.6 ± 0.3) nm (inset), and the dynamic light scattering analysis showing a hydrodynamic diameter (HD) of (3.0 ± 0.4) nm in aqueous solution. d) The absorption (blue), excitation (green), and emission (red) spectra of GS-[^{198}Au]AuNPs in aqueous solution.

Physiological stability of imaging probes is critically important for their biomedical application. To evaluate the stability of GS-[^{198}Au]AuNPs, we measured the fluorescence and SPECT signals of the NPs at both in vitro and in vivo levels. Figure S3 shows the luminescence spectra of the GS-[^{198}Au]AuNPs incubated in water, phosphate buffered saline (PBS), and PBS containing 10% fetal bovine serum (FBS) at 37 °C for 48 h. Little changes in the emission intensities and spectra suggested the GS-[^{198}Au]AuNPs were fairly stable under these conditions. In addition, based on radio-HPLC assay measurements (Figure S4), the retention time of the NPs was 6.5 min in both water and PBS, but in PBS containing 10% FBS, an additional component with 5.8 min retention time (15%) was observed. These retention times are different from that (10.2 min) of free ^{198}Au ions, indicating no ^{198}Au dissociation under these conditions. The additional component with retention time of 5.8 min might be due to the association to serum proteins as this component remained fluorescent in the gel electrophoresis studies (Figure S5). The in vivo stability of GS-[^{198}Au]AuNPs was further evaluated by examining the fluorescence spectroscopy and radio-HPLC profiles of the excreted radioactivities in the collected urine (Figure S6). Impressively, little change was observed before and after the particle circulation in mice. This unequivocally indicates the integrity of the GS-[^{198}Au]AuNPs during the in vivo circulation. Interestingly, nearly 12% of the GS-[^{198}Au]AuNPs were also found in association with serum proteins as determined by size-exclusive radio-HPLC analysis, which are consistent with the in vitro results.

The pharmacokinetic parameters of GS-[^{198}Au]AuNPs were measured in normal balb/c mice (see the Supporting Information for a detailed procedure). The results showed that the GS-[^{198}Au]AuNPs exhibited a two-compartment profile of in vivo kinetics with a $t_{1/2\alpha}$ of 5.0 min and a $t_{1/2\beta}$ of 12.7 h (Figure 2a). The short $t_{1/2\alpha}$ of GS-[^{198}Au]AuNPs indicates that these NPs can rapidly distribute into tissues during the circulation, similar to those of reported molecular imaging agents such as ^{99m}Tc-labeled MAb ior egf/r3 (8.2 min)[16] and ^{64}Cu-labeled DOTA-NHGR$_{11}$ (10.7 min)[19] but different from

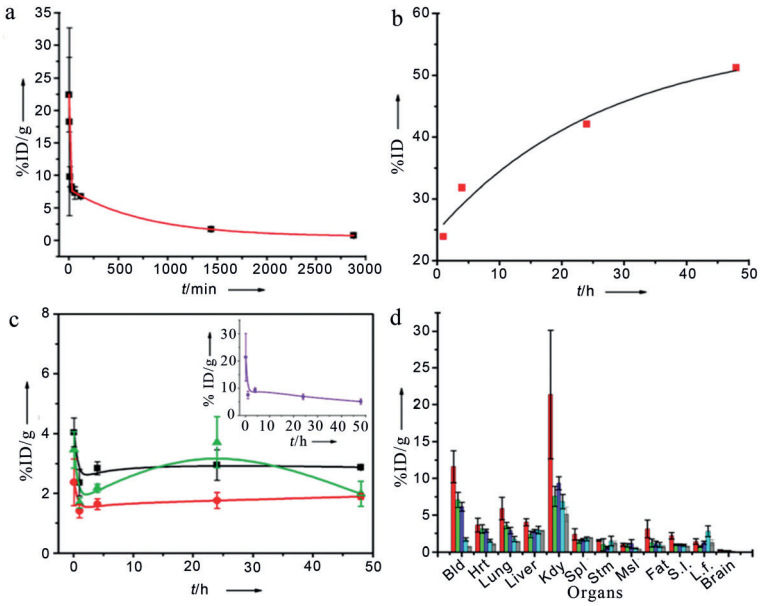

Figure 2. Biodistribution and pharmacokinetics of GS-[^{198}Au]AuNPs in normal balb/c mice. a) The time–activity curve (TAC) of GS-[^{198}Au]AuNPs in blood. The pharmacokinetic parameters were determined by fitting the data with a two-compartment model. b) Excretion of GS-[^{198}Au]AuNPs in the urine at 1, 4, 24, and 48 h p.i. c) TACs of GS-[^{198}Au]AuNPs in liver (black), spleen (red), intestines (green), and kidneys (inset). d) Biodistribution of GS-[^{198}Au]AuNPs 5 min (red), 1 h (green), 4 h (blue), 24 h (cyan), and 48 h (grey) p.i. (Bld: blood, Hrt: heart, Kdy: kidney, Spl: spleen, Stm: stomach, Msl: muscle, S.I.: small intestine, and L.I.: large intestine; %ID/g = percentage of the injected dose per gram of tissue).

NPs-based agents such as bovine-serum-albumin-coated and mercaptoundecanoic-acid-coated quantum dots (QDs) with a single half-life of about 0.65 h and 0.98 h, respectively.[14a] The relatively long $t_{1/2\beta}$ of GS-[^{198}Au]AuNPs is comparable to the $t_{1/2\beta}$ (about 17.2 h) of ^{64}Cu-labeled DOTA-NHGR$_{11}$,[19] further indicating that GS-[^{198}Au]AuNPs indeed behaved like small molecular probes in pharmacokinetics.

More than 50% of GS-[^{198}Au]AuNPs were cleared out of the body after 48 h (Figure 2b), indicating that these radioactive NIR-emitting AuNPs are renal clearable. Biodistributions of GS-[^{198}Au]AuNPs in kidney, liver, spleen and intestines at 5 min, 1, 4, 24, and 48 h after IV injection also provide additional insights on the clearance pathways and kinetics (Figure 2c). While the pharmacokinetic profile of the NPs varies with organs, one common feature is that the highest accumulation of the NPs occurred within 5 min p.i. followed by efficient clearance. This observation is consistent with the measured short $t_{1/2\alpha}$, indicating that the tissue distribution of the NPs was indeed rapid. The highest uptake of GS-[^{198}Au]AuNPs in the kidney was followed by a gradual decrease from about 21% of the injected dose per gram (ID/g) to about 5% of ID/g (inset of Figure 2c), which was in agreement with the clearance of the NPs from blood (Figure 2a), indicating that the NPs were mainly excreted through the glomerular filtration. While the rapid decreases of the particle concentrations in the liver, spleen, and intestines in the first hour was due to re-entrance of the NPs into the blood, these organs indeed provide additional clearance pathways. Interestingly, the accumulations of the NPs in the liver and spleen roughly remained constant even though the NPs were still circulating in the blood, indicating the slow clearance of the NPs through a hepatic route. The uptake level of the GS-[^{198}Au]AuNPs in intestines varied with time, reaching its maximum (about 3.7% of ID/g) at 24 h p.i. and then decreasing to about 1.9% of ID/g after 48 h p.i., suggesting that a small amount of GS-[^{198}Au]AuNPs can be cleared out of the body through the metabolism route in addition to the urinary system. The detailed biodistribution data (see the Supporting Infromation for the detailed procedure) of the GS-[^{198}Au]AuNPs in other organs were summarized in Figure 2d and Table S1. The accumulation of the NPs in heart, lung, muscle, and fat also decreased with time, indicating that the GS-[^{198}Au]AuNPs were only temporally distributed to these tissues because of the rapid adsorption process and could be efficiently washed away within the first 48 h without causing an uptake increase in the liver and spleen. The origin of the resulted biodistribution and efficient renal clearance of the NPs were attributed to the small particle size and glutathione ligand, which enable the GS-[^{198}Au]AuNPs highly stable in the physiological environment and resistant to serum protein adsorption.[15b] As a result, the hydrodynamic diameter of the NPs in the body was still below the size threshold for renal clearance and the NPs remained stealthy to RES organs.

The ^{198}Au in these GS-[^{198}Au]AuNPs not only helps to quantify the pharmacokinetics of these NIR-emitting AuNPs rapidly, but also offers a potential opportunity for in vivo SPECT imaging by emitting gamma rays. ^{198}Au is a radioisotope with a relative long half-life of 2.7 days and gamma emission energy at 0.411 MeV. To further demonstrate the potential SPECT application of these GS-[^{198}Au]AuNPs, we performed a SPECT imaging evaluation in balb/c mice IV injected with about 37 MBq ($\approx$100 μL) of the NPs at 10 min, 1, 4, and 24 h p.i. Shown in Figure 3a, the mouse kidneys and bladder can be clearly seen on SPECT images after 10 min p.i., consistent with the results obtained from the pharmacokinetics studies. After that, the SPECT signals gradually decreased in the kidneys, but remained high in the bladder, indicating the renal clearance of GS-[^{198}Au]AuNPs (Figure 3b and c). Significant reduction in the signals was found in the kidneys and bladder after 24 h p.i. (Figure 3d), suggesting that the majority of GS-[^{198}Au]AuNPs was eliminated through urine within 24 h p.i., consistent with the obtained pharmacokinetic parameters ($t_{1/2\beta}$ = 12.7 h).

While SPECT is capable of deep tissue imaging and quantification, its low temporal resolution often hampers its application to visualization of dynamic processes, where fluorescence imaging technique can definitely play a complementary role. Using NIR emission of GS-[^{198}Au]AuNPs, we quantified the pharmacokinetics of GS-[^{198}Au]AuNPs in the bladder in the first 20 min at a higher temporal resolution

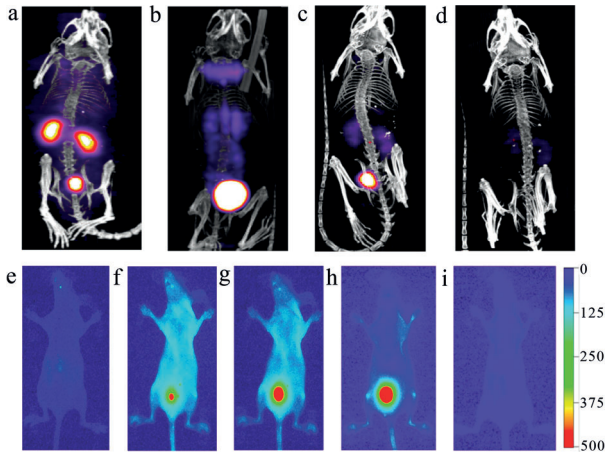

Figure 3. Representative SPECT images (top row) of balb/c mice injected with GS-[^{198}Au]AuNPs. a) 10 min, b) 1 h, c) 4 h, and d) 24 h p.i. In vivo fluorescence imaging (bottom row) of a live mouse e) pre-injection, f) 5 min, g) 20 min, h) 1 h, and i) 24 h after IV injection of GS-[^{198}Au]AuNPs.

(Figure 3e–g) and found first-order in vivo kinetics with a half-life of 3.8 min (Figure S7), similar to small-molecule contrast agents in terms of their pharmacokinetic parameters.[20] In addition, direct comparison between fluorescence (Figure 3h&i) and SPECT (Figure 3b&d) imaging at 1 and 24 h p.i. show the same distribution kinetics of GS-[^{198}Au]AuNPs in the bladder.

In summary, we have demonstrated a one-step synthesis of NIR-emitting radioactive AuNPs, which were incorporated with a gold radioisotope ^{198}Au. These GS-[^{198}Au]AuNPs are renal clearable and exhibit rapid in vivo kinetics comparable to small-molecule contrast agents in clinical practice. We acknowledge that the gamma emission energy of ^{198}Au is beyond the optimum energy detection window of current SPECT imaging systems. This problem can be potentially resolved by using radioisotopes emitting lower gamma energies than ^{198}Au, for instance ^{199}Au ($t_{1/2} = 3.14$ d; $\gamma =$ 159.6 keV)[17a] or modifying the hardware of the scanner such as the aperture design. More importantly, our work suggests a feasible approach to optimize the in vivo kinetics of NPs for future clinical applications by using well-established surface chemistry. Of note, we focused on pharmacokinetics at the first 48 h p.i. in this study and about 50% of the GS-[^{198}Au]AuNPs were cleared out of the body through urine. Since ideal clinical probes should be completely excreted from the body and pose minimal in vivo toxicity, the long-term toxicity of GS-[^{198}Au]AuNPs need to be further evaluated before practical applications. The pharmacokinetics of these NIR-emitting radioactive AuNPs renders the NPs with potential applications as dual-modality imaging probes for fluorescence and SPECT imaging techniques. Further functionalization will enable these molecular nanoprobes to target diseases more specifically, which is under investigation.

Received: April 19, 2012
Revised: July 27, 2012
Published online: September 7, 2012

Keywords: gold · imaging agents · luminescence · nanoparticles · pharmacokinetics

[1] B. D. R. Weissleder, A. Rehemtulla, S. Sam Gambhir, *Molecular Imaging: Principles and Practice*, 1st ed., Pmph Usa, **2010**.
[2] T. W. Ohtake, T. Kosaka, N. Momose, T. Nishikawa, J. Sasaki, Y. Lio, M. Saihara, S. Suqimoto, *Kaku Igaku* **1991**, *28*, 71–82.
[3] R. S. Liu, T. K. Chou, C. H. Chang, C. Y. Wu, C. W. Chang, T. J. Chang, S. J. Wang, W. J. Lin, H. E. Wang, *Nucl. Med. Biol.* **2009**, *36*, 305–312.
[4] V. Lorusso, P. Taroni, S. Alvino, A. Spinazzi, *Invest. Radiol.* **2001**, *36*, 309–316.
[5] a) W. J. Rieter, J. S. Kim, K. M. L. Taylor, H. An, W. Lin, T. Tarrant, W. Lin, *Angew. Chem.* **2007**, *119*, 3754–3756; *Angew. Chem. Int. Ed.* **2007**, *46*, 3680–3682; b) K. M. L. Taylor, A. Jin, W. Lin, *Angew. Chem.* **2008**, *120*, 7836–7839; *Angew. Chem. Int. Ed.* **2008**, *47*, 7722–7725; c) J. F. Lovell, C. S. Jin, E. Huynh, H. Jin, C. Kim, J. L. Rubinstein, W. C. W. Chan, W. Cao, L. V. Wang, G. Zheng, *Nat. Mater.* **2011**, *10*, 324–332; d) S. R. Banerjee, M. Pullambhatla, Y. Byun, S. Nimmagadda, C. A. Foss, G. Green, J. J. Fox, S. E. Lupold, R. C. Mease, M. G. Pomper, *Angew. Chem.* **2011**, *123*, 9333–9336; *Angew. Chem. Int. Ed.* **2011**, *50*, 9167–9170; e) M. Swierczewska, S. Lee, X. Y. Chen, *Mol. Imaging* **2011**, *10*, 3–16.
[6] a) S. Mizukami, R. Takikawa, F. Sugihara, M. Shirakawa, K. Kikuchi, *Angew. Chem.* **2009**, *121*, 3695–3697; *Angew. Chem. Int. Ed.* **2009**, *48*, 3641–3643; b) C. Tu, R. Nagao, A. Y. Louie, *Angew. Chem.* **2009**, *121*, 6669–6673; *Angew. Chem. Int. Ed.* **2009**, *48*, 6547–6551.
[7] a) E. C. Cho, C. Glaus, J. Chen, M. J. Welch, Y. Xia, *Trends Mol. Med.* **2010**, *16*, 561–573; b) S. Wang, B. R. Jarrett, S. M. Kauzlarich, A. Y. Louie, *J. Am. Chem. Soc.* **2007**, *129*, 3848–3856; c) Y. D. Jin, X. H. Gao, *Nat. Nanotechnol.* **2009**, *4*, 571–576; d) R. Hao, R. J. Xing, Z. C. Xu, Y. L. Hou, S. Gao, S. H. Sun, *Adv. Mater.* **2010**, *22*, 2729–2742; e) W. B. Cai, X. Y. Chen, *J. Nucl. Med.* **2008**, *49*, 113S–128S; f) J.-H. Lee, K. Lee, S. H. Moon, Y. Lee, T. G. Park, J. Cheon, *Angew. Chem.* **2009**, *121*, 4238–4243; *Angew. Chem. Int. Ed.* **2009**, *48*, 4174–4179; g) L. Cheng, K. Yang, Y. G. Li, J. H. Chen, C. Wang, M. W. Shao, S. T. Lee, Z. Liu, *Angew. Chem.* **2011**, *123*, 7523–7528; *Angew. Chem. Int. Ed.* **2011**, *50*, 7385–7390; h) Q. Liu, M. Chen, Y. Sun, G. Chen, T. Yang, Y. Gao, X. Zhang, F. Li, *Biomaterials* **2011**, *32*, 8243–8253.
[8] W. B. Cai, K. Chen, Z. B. Li, S. S. Gambhir, X. Y. Chen, *J. Nucl. Med.* **2007**, *48*, 1862–1870.
[9] a) D. Boyer, P. Tamarat, A. Maali, B. Lounis, M. Orrit, *Science* **2002**, *297*, 1160–1163; b) J. L. West, N. J. Halas, *Annu. Rev. Biomed. Eng.* **2003**, *5*, 285–292; c) J. Y. Chen, B. Wiley, Z. Y. Li, D. Campbell, F. Saeki, H. Cang, L. Au, J. Lee, X. D. Li, Y. N. Xia, *Adv. Mater.* **2005**, *17*, 2255–2261; d) X. H. Huang, I. H. El-Sayed, W. Qian, M. A. El-Sayed, *J. Am. Chem. Soc.* **2006**, *128*, 2115–2120; e) P. K. Jain, X. H. Huang, I. H. El-Sayed, M. A. El-Sayed, *Acc. Chem. Res.* **2008**, *41*, 1578–1586; f) R. Hu, K. T. Yong, I. Roy, H. Ding, S. He, P. N. Prasad, *J. Phys. Chem. C* **2009**, *113*, 2676–2684; g) C. Zhou, J. Yu, Y. Qin, J. Zheng, *Nanoscale* **2012**, *4*, 4228–4233.
[10] a) D. Kim, S. Park, J. H. Lee, Y. Y. Jeong, S. Jon, *J. Am. Chem. Soc.* **2007**, *129*, 7661–7665; b) X. M. Yang, S. E. Skrabalak, Z. Y. Li, Y. N. Xia, L. H. V. Wang, *Nano Lett.* **2007**, *7*, 3798–3802; c) Q. Y. Cai, S. H. Kim, K. S. Choi, S. Y. Kim, S. J. Byun, K. W. Kim, S. H. Park, S. K. Juhng, K. H. Yoon, *Invest. Radiol.* **2007**,

42, 797 – 806; d) S. Mallidi, T. Larson, J. Tam, P. P. Joshi, A. Karpiouk, K. Sokolov, S. Emelianov, *Nano Lett.* **2009**, *9*, 2825 – 2831; e) C. Kim, E. C. Cho, J. Y. Chen, K. H. Song, L. Au, C. Favazza, Q. A. Zhang, C. M. Cobley, F. Gao, Y. N. Xia, L. H. V. Wang, *ACS Nano* **2010**, *4*, 4559 – 4564; f) Y. Jin, C. Jia, S.-W. Huang, M. O'Donnell, X. Gao, *Nat. Commun.* **2010**, *1*, 41.

[11] P. Cherukuri, C. J. Gannon, T. K. Leeuw, H. K. Schmidt, R. E. Smalley, S. A. Curley, R. B. Weisman, *Proc. Natl. Acad. Sci. USA* **2006**, *103*, 18882 – 18886.

[12] H. L. Ma, Y. F. Xu, X. R. Qi, Y. Maitani, T. Nagai, *Int. J. Pharm.* **2008**, *354*, 217 – 226.

[13] a) X. H. Gao, Y. Y. Cui, R. M. Levenson, L. W. K. Chung, S. M. Nie, *Nat. Biotechnol.* **2004**, *22*, 969 – 976; b) A. K. Gupta, M. Gupta, *Biomaterials* **2005**, *26*, 3995 – 4021; c) W. H. De Jong, W. I. Hagens, P. Krystek, M. C. Burger, A. J. A. M. Sips, R. E. Geertsma, *Biomaterials* **2008**, *29*, 1912 – 1919.

[14] a) H. C. Fischer, L. C. Liu, K. S. Pang, W. C. W. Chan, *Adv. Funct. Mater.* **2006**, *16*, 1299 – 1305; b) W. H. Liu, H. S. Choi, J. P. Zimmer, E. Tanaka, J. V. Frangioni, M. Bawendi, *J. Am. Chem. Soc.* **2007**, *129*, 14530 – 14531; c) H. S. Choi, W. H. Liu, F. B. Liu, K. Nasr, P. Misra, M. G. Bawendi, J. V. Frangioni, *Nat. Nanotechnol.* **2010**, *5*, 42 – 47; d) H. A. Xie, Z. J. Wang, A. D. Bao, B. Goins, W. T. Phillips, *Int. J. Pharm.* **2010**, *395*, 324 – 330; e) F. Lux, A. Mignot, P. Mowat, C. Louis, S. Dufort, C. Bernhard, F. Denat, F. Boschetti, C. Brunet, R. Antoine, P. Dugourd, S. Laurent, L. Vander Elst, R. Muller, L. Sancey, V. Josserand, J. L. Coll, V. Stupar, E. Barbier, C. Remy, A. Broisat, C. Ghezzi, G. Le Duc, S. Roux, P. Perriat, O. Tillement, *Angew. Chem.* **2011**, *123*, 12507 – 12511; *Angew. Chem. Int. Ed.* **2011**, *50*, 12299 – 12303.

[15] a) C. Zhou, C. Sun, M. X. Yu, Y. P. Qin, J. G. Wang, M. Kim, J. Zheng, *J. Phys. Chem. C* **2010**, *114*, 7727 – 7732; b) C. Zhou, M. Long, Y. P. Qin, X. K. Sun, J. Zheng, *Angew. Chem.* **2011**, *123*, 3226 – 3230; *Angew. Chem. Int. Ed.* **2011**, *50*, 3168 – 3172; c) M. X. Yu, C. Zhou, J. B. Liu, J. D. Hankins, J. Zheng, *J. Am. Chem. Soc.* **2011**, *133*, 11014 – 11017.

[16] N. Iznaga-Escobar, L. A. T. Arocha, A. M. Morales, M. R. Suzarte, N. R. Mesa, R. P. Rodriguez, *J. Nucl. Med.* **1998**, *39*, 1918 – 1927.

[17] a) C. E. Floyd, R. J. Jaszczak, C. C. Harris, R. E. Coleman, *Phys. Med. Biol.* **1984**, *29*, 1217 – 1230; b) P. Ritt, H. Vija, J. Hornegger, T. Kuwert, *Eur. J. Nucl. Med. Mol. Imaging* **2011**, *38*, 69 – 77.

[18] a) J. Zheng, C. Zhou, M. Yu, J. Liu, *Nanoscale* **2012**, *4*, 4073 – 4083; b) X. J. Tu, W. B. Chen, X. Q. Guo, *Nanotechnology* **2011**, *22*, 095701; c) L. Shang, R. M. Dorlich, S. Brandholt, R. Schneider, V. Trouillet, M. Bruns, D. Gerthsen, G. U. Nienhaus, *Nanoscale* **2011**, *3*, 2009 – 2014; d) C. L. Liu, H. T. Wu, Y. H. Hsiao, C. W. Lai, C. W. Shih, Y. K. Peng, K. C. Tang, H. W. Chang, Y. C. Chien, J. K. Hsiao, J. T. Cheng, P. T. Chou, *Angew. Chem.* **2011**, *123*, 7194 – 7198; *Angew. Chem. Int. Ed.* **2011**, *50*, 7056 – 7060.

[19] G. Y. Hao, J. Zhou, Y. Guo, M. A. Long, T. Anthony, J. Stanfield, J. T. Hsieh, X. K. Sun, *Amino Acids* **2011**, *41*, 1093 – 1101.

[20] K. O. Vasquez, C. Casavant, J. D. Peterson, *Plos One* **2011**, *6*, e20594.

